Ordering Dynamics of Compositionally Asymmetric Styrene−Isoprene Block Copolymers

J. LaMonte Adams, Daniel J. Quiram, William W. Graessley, and Richard A. Register*

Department of Chemical Engineering, Princeton University, Princeton, New Jersey 08544

Gary R. Marchand

The Dow Chemical Company, P.O. Box 400, Plaquemine, Louisiana 70765

Received August 28, 1995; Revised Manuscript Received January 15, 1996[⊗]

ABSTRACT: We investigate the development of mesophase order in compositionally asymmetric (13 wt % styrene) polystyrene−polyisoprene (SI) diblock and SIS triblock copolymers. The equilibrium ordered morphology of these polymers is a body-centered-cubic (bcc) lattice of spherical S microdomains. The ordering kinetics are measured by quenching the material from above the order−disorder transition temperature (T_{ODT}) to a temperature where the ordered phase is stable and following the structure development by time-resolved small-angle X-ray scattering and dynamic oscillatory rheological measurements. The kinetics are significantly slower than those observed for nearly symmetric polymers of similar T_{ODT}, resulting in a wider range of experimentally accessible quench depths. The temporal evolution of the storage modulus G' measured at constant frequency displays a two-step increase after a quench from above the ODT, for sufficiently low temperatures and/or high molecular weights. The long-time step corresponds to the development of a bcc lattice of spherical microdomains, while the first step results from the finite time required for large-amplitude composition fluctuations to develop fully.

I. Introduction

The order−disorder transition (ODT) in block copolymers has received considerable attention over the past two decades. Leibler[1] used a mean-field approach to express the ODT, *i.e.* the phase boundary dividing the ordered mesophases from the disordered state, for AB diblock copolymers in terms of the volume fraction of A units f and the product χN, where χ is the Flory interaction parameter and N is the total number of monomer units in the block copolymer. Leibler's theory has been extended to triblock copolymers by Mayes and Olvera de la Cruz.[2] These approaches predict the existence of a spinodal curve with the region between the ODT (binodal at $(\chi N)_{ODT}$) and spinodal (at $(\chi N)_S$) curves representing a metastable region in which the block copolymers are expected to order by a nucleation and growth mechanism. According to Leibler's mean-field approach, the microphase separation process should proceed via spinodal decomposition[1] for values of χN greater than $(\chi N)_S$. When the mean-field calculations are corrected for composition fluctuations that have been observed experimentally in the disordered region, the existence of a spinodal curve is no longer predicted,[3] indicating that ordering should always proceed via nucleation and growth.[4,5]

Many studies utilizing rheology[6−11] and small-angle X-ray or neutron scattering (SAXS or SANS)[11−14] have concentrated on determining the ODT temperature (T_{ODT}) and investigating the behavior of block copolymers both above and below T_{ODT}. The rheological signature of the ODT is an abrupt change in the slope of a plot of the dynamic storage modulus G' vs T, while in SAXS or SANS, the signature is an abrupt increase in width of the primary peak. Several studies have investigated block copolymer ordering kinetics in the region where χN slightly exceeds $(\chi N)_{ODT}$. Rosedale and Bates,[9] using rheology on a nearly symmetric (f_{EP} = 0.55) poly(ethylene-*alt*-propylene)−poly(ethylethylene) diblock, observed a small temperature window (∼7 °C) below T_{ODT} over which the ordering process occurred on a measurable time scale after a quench from the disordered state. Similar results were reported by Floudas *et al.*[15] for a nearly symmetric (f_S = 0.51) polystyrene−polyisoprene (SI) diblock for quench depths up to ∼11 °C, as well as for miktoarm star polymers to slightly greater quench depths.[16] Both groups observed a decrease in the ordering time with increasing ΔT. Stühn and co-workers[17,18] and Hashimoto and Sakamoto[19] performed similar experiments employing time-resolved SAXS to study the ordering kinetics of other nearly symmetric (f_S = 0.44) SI diblocks.

There have been fewer investigations on asymmetric systems. Schuler and Stühn[17] used time-resolved SAXS to examine the ordering kinetics of a polystyrene-rich (f_S = 0.77) SI diblock; for their polymer, however, T_{ODT} and the glass transition temperature of the polystyrene block were in close proximity, leading to a strong coupling between the two. Winter *et al.*[20] used time-resolved rheology and SAXS to investigate the development of a hexagonally packed cylindrical morphology of an SIS triblock (f_S = 0.24) and found that the ordering rate as perceived by SAXS was an order of magnitude faster than that perceived rheologically.

Several studies have also explored the ordering process in concentrated block copolymer solutions, as opposed to undiluted melts. Hashimoto[21] used time-resolved SAXS to probe the ordering of a symmetric polystyrene−polybutadiene−polystyrene (SBS) triblock dissolved in the nonselective solvent dipentene for a quench depth ($\Delta T \equiv T_{ODT} - T$) of 130 °C. A series of investigations[22−26] have been performed on an SB diblock (f_S = 0.30) dissolved in *n*-tetradecane, which is a selective solvent for polybutadiene. Polystyrene spheres were formed which ordered onto a body-centered-cubic (bcc) lattice. Singh and co-workers[23−25] investigated the ordering kinetics via time-resolved SAXS for solutions

* To whom correspondence should be addressed.
[⊗] Abstract published in *Advance ACS Abstracts,* March 15, 1996.

0024-9297/96/2229-2929$12.00/0

Table 1. Polymer Characterization

			T_{ODT} (°C)	
polymer	wt % styrene	M_w (kg/mol)	rheology	SAXS
D62	13.0	62.6	110 ± 2	111 ± 2
D78	13.5	78.4	156 ± 2	161 ± 2
D90	13.1	90.6	197 ± 2	202 ± 2
T149	13.0	149.0	164 ± 2	167 ± 2

of varying composition, while Shannon *et al.*[26] doped these solutions with impurities to compare the kinetics arising from homogeneous and heterogeneous nucleation. How these studies on block copolymer solutions translate to the undiluted melt is presently unclear.

Asymmetric block copolymers, particularly triblocks, are of great practical interest as thermoplastic elastomers and hot-melt adhesives.[27] However, we have found no experimental reports on the ordering kinetics for highly asymmetric block copolymers (*i.e.*, materials forming spheres in the ordered state) in bulk. Moreover, there appears to be only a single literature report on the ordering behavior of a triblock copolymer in bulk,[20] and no comparison was made with analogous diblocks. Full development of the equilibrium structure obviously demands processing times which are at least as long as the time required for ordering, yet the ordering rates in such materials are essentially unknown at present. Here we employ both rheological and time-resolved SAXS measurements to monitor the ordering kinetics of SI diblock and SIS triblock copolymers, all with $f_S = 0.11$ and ranging in molecular weight from 62 to 149 kg/mol. Comparisons are made with the ordering behavior reported for symmetric block copolymers.

II. Experimental Section

A. Materials. The SI diblock and SIS triblock copolymers used in this study (Table 1) were synthesized and characterized by DEXCO Polymers and have been described previously.[6] In the sample code, "D" and "T" indicate the architecture (diblock or triblock), while the digits are the polymer molecular weight in kg/mol. The isoprene block is high (93%) in 1,4 content. The polydispersity (M_w/M_n) is less than 1.03 for all polymers, as determined by gel permeation chromatography (GPC). GPC analysis following rheological or X-ray measurements revealed only minor amounts (<10%) of chain scission and branching after exposure to 150 °C for several days. The glass transition temperature T_g of the polystyrene phase, which we could not detect by differential scanning calorimetry, is estimated to be less than 70 °C for all of the block copolymers studied based on the literature.[28]

B. Rheology. Values of T_{ODT} for these polymers obtained via rheological measurements were reported previously.[6] Since then, we have replaced our Rheometrics System IV rheometer with a Rheometrics RMS-800, which provides better temperature control and an order of magnitude improvement in torque resolution. Samples for rheological testing were prepared by compression molding. Parallel-plate geometry (25 mm diameter) was used to obtain the dynamic storage and loss moduli, $G'(\omega)$ and $G''(\omega)$, over the frequency range $10^{-2} < \omega < 10^2$ rad/s. With the exception of the work presented in Figure 3, a 5% strain amplitude was employed. Values for T_{ODT} using the RMS-800 are slightly higher (by 4 ± 2 °C) than those reported earlier[6] (see Table 1). The temperature resolution of the RMS-800 is ±1 °C; the environmental chamber was continuously flushed with nitrogen to minimize thermal and oxidative degradation. For the kinetic ordering studies, the materials were first heated to at least 10 °C above T_{ODT} and held there for 15 min. The temperature was then quickly lowered to a specified temperature below T_{ODT}. Though the initial temperature drop is quite rapid, approximately 3 min was required for the rheometer oven temperature to stabilize; the time at which the rheometer was commanded to begin the quench is designated as the zero time for the ordering kinetics measurements. Subsequently, the temporal evolution of G' and G'' was monitored at constant ω. Since the rheometer oven and sample temperatures are not identical during thermal transients, analogous quench studies were performed on a silicone oil; its modulus rose to within 1% of its asymptotic limit within 5 min of the start of the quench (i.e., roughly 2 min after the rheometer oven temperature had stabilized).

C. SAXS. ODT temperatures were measured by SAXS through the use of a recently constructed hot stage equipped with a resistive heater. Samples were enclosed in copper cells, bounded on both sides by 0.8 mil thick V4 grade mica (Asheville-Schoonmaker Mica Co., Newport News, VA). SAXS data were collected with a compact Kratky camera connected to a one-dimensional Braun position-sensitive detector. The data were reduced using previously reported procedures[29] to desmeared absolute intensity versus the scattering vector $q = (4\pi/\lambda) \sin \theta$, where λ is the radiation wavelength and 2θ is the scattering angle. Over the temperature range studied, the precision of the hot stage temperature control was found to be ±1 °C. Evacuation of the camera reduced both spurious scattering from air and oxidative degradation of the samples.

In the SAXS kinetic experiments, the materials were first heated to at least 10 °C above T_{ODT}. Once thermal equilibrium was achieved, a scattering profile was collected. This was succeeded by a reduction in temperature to a specified value below T_{ODT}. The sample reached thermal equilibrium within 15 min for the largest quench depth investigated; the time at which the sample reached temperature is designated as the zero time for the ordering kinetics measurements. Scattering profiles were then taken continuously; counts for each scattering profile were accumulated for 10, 20, or 30 min, depending on the time scale of the particular kinetic experiment. The different cooling rates between the rheometer and the SAXS hot stage and consequent differences in zero time might be expected to lead to some systematic differences in ordering rates as measured by the two techniques; however, these discrepancies should be less than the thermal equilibration time (<15 min), which is considerably shorter than the half-times measured by SAXS, and thus comparisons between the two techniques remain valid.

III. Results

A. ODT Determination. SAXS patterns for all four block copolymers studied here (as well as the other four investigated in our previous paper[6]), collected on compression-molded disks prior to rheological testing, reveal considerable disorder[6] (see lower curve in Figure 13 for an example). These SAXS patterns can be quantitatively fit by a model wherein the spherical polystyrene microdomains adopt a liquid-like arrangement within the polyisoprene matrix[30] (see Discussion for further details). We had previously[6] assumed that the liquid-like packing of spheres, inferred from the SAXS data on compression-molded samples, persisted up to the observed rheological transition. However, using high-temperature SAXS, we have found that annealing these polymers between the polystyrene T_g and T_{ODT} allows the equilibrium bcc morphology to develop in some cases. This annealing is most effective when $T_{ODT} \gg T_g$ and is accelerated when the polymer chains are short. Those materials which adopt a bcc lattice during heating below T_{ODT} show sharper rheological transitions at the ODT than those which do not. Thus T149, D90, D78, and D62 adopt the bcc structure rapidly (as seen by SAXS) and show sharp rheological transitions.[6] By contrast, the four other polymers which were also part of our initial work[6] adopt the bcc lattice only after annealing for extended periods (several days for T120) if at all (we have not found conditions which produce bcc order in T107, T90, and D48). We are concerned here only with the four polymers which rapidly adopt the bcc lattice.

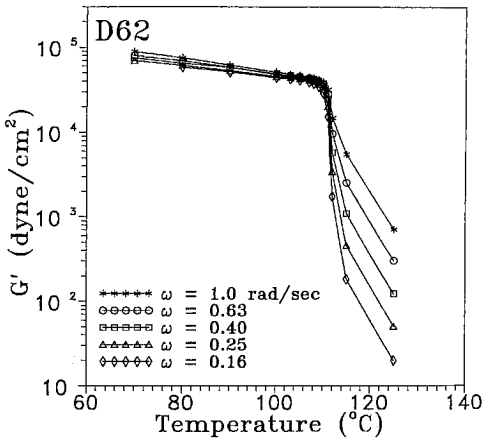

Figure 1. Isochronal plots of G' vs temperature for the diblock D62 in the vicinity of T_{ODT} (110 ± 2 °C) at various frequencies ω. The transition (abrupt change in slope) becomes sharper with decreasing ω (i.e., for values of $\omega\tau_d \ll 1$, where τ_d is the terminal relaxation time of the polymer in the disordered state).

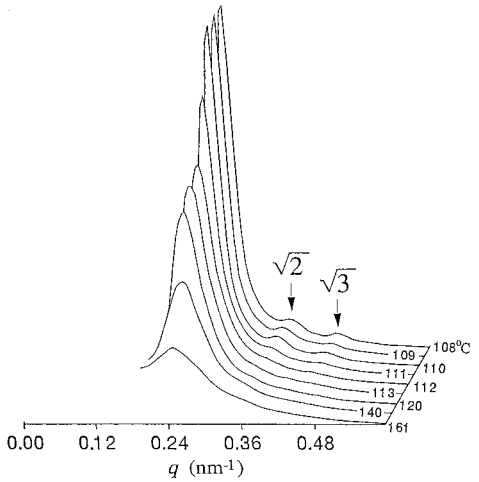

Figure 2. SAXS data for the ODT determination for the diblock D62. Vertical intensity axis is linear; sample temperatures are indicated on curves. For temperatures of 110 °C and below, note the presence of three narrow reflections in q ratios of 1:√2:√3, indicating a cubic structure which we assign to a bcc packing of spheres. At 112 °C and above, note that only a single broad peak is present, indicating $T_{ODT} = 111 \pm 2$ °C. Near T_{ODT}, curves are shown in 1 °C increments; three additional curves, at 120, 140, and 161 °C, are shown to emphasize that scattering from the homogeneous phase is easily detectable to temperatures 50 °C above T_{ODT}.

Figures 1 and 2 show representative rheological and SAXS data used to determine T_{ODT}. From the abrupt slope change in G' vs T plots for D62 (Figure 1), we obtain $T_{ODT} = 110 \pm 2$ °C. The SAXS data for the same sample (Figure 2) show a simultaneous decrease in primary peak height and increase in peak width along with the disappearance of the higher order maxima at 111 ± 2 °C, corresponding to T_{ODT}. The rheological and X-ray measurements agree to within 5 °C in all cases (see Table 1).

B. Ordering Kinetics (Rheology). The isochronal frequency used in these measurements must meet two criteria: it must be low enough that the mesophase structure dominates the rheological response,[9] while being high enough to provide adequate time resolution (each point is acquired over a $2\pi/\omega$ period). The frequency used in the studies, $\omega = 0.04$ rad/s, satisfied both these criteria. The effect of imposed strain amplitude γ_o at $\omega = 0.04$ rad/s was investigated over the range 0.02−0.15, using sample D78 and a quench depth

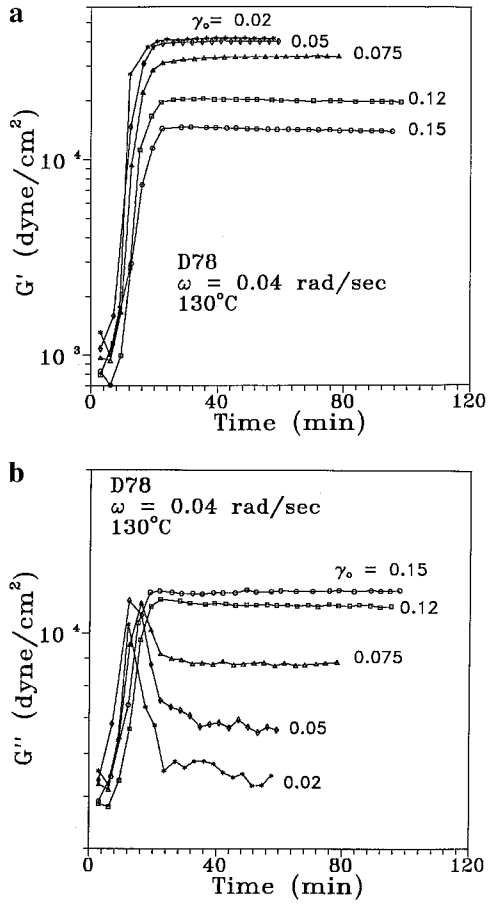

Figure 3. Effect of strain amplitude γ_o on the ordering behavior as measured by G' (a) and G'' (b) for the diblock D78 at 130 °C and $\omega = 0.04$ rad/s. Note the change in curve shape for G'' between $\gamma_o = 0.075$ and $\gamma_o = 0.12$.

$\Delta T = 26$ °C. Surprisingly, although the magnitude of the modulus exhibits a noticeable strain dependence above 0.05 strain units (see Figure 3a), the shape of the ordering curve and the total time required for G' to reach its equilibrium value are essentially independent of γ_o. The changes in G'' with increasing γ_o (see Figure 3b) are more noticeable; at $\gamma_o = 0.12$ and above, G'' no longer displays a maximum, but instead has a shape analogous to that displayed by G'. This behavior is reversible; both moduli recovered 95% of their low-strain values within 15 min after γ_o was reduced from 0.15 to 0.02 at 130 °C. These observations suggest that the lattice structure is severely distorted and perhaps even destroyed under shear of sufficiently large strain amplitude. Similar conclusions were drawn by Koppi *et al.*[31] For the remainder of the work presented here, a 5% strain amplitude was employed; while Figure 3b shows that this strain actually exceeds the linear viscoelastic limit (which evidently is restricted to quite small strains in these ordered block copolymers), our principal interest is in the ordering rate, which Figure 3a shows to be substantially unaffected by strain amplitude.

Figure 4 shows the temporal evolution of G' and G'' for D78 at several temperatures. The shapes of these curves are similar to what has been reported for other systems.[9,15,20] The time required for the modulus to reach its equilibrium value decreases with decreasing temperature (increasing ΔT), with a minimum in the ordering time occurring between 110 and 140 °C. We assume the minimum results from the competition between an increasing thermodynamic driving force for phase separation with decreasing T (χ increases with

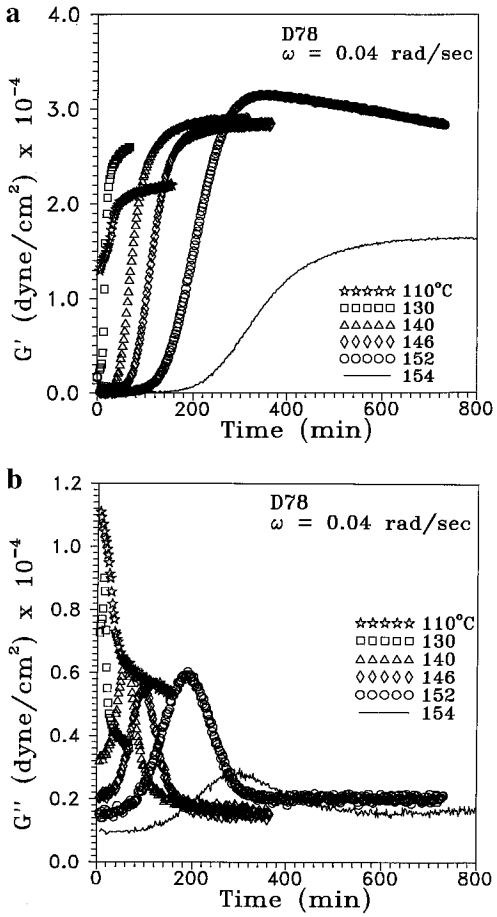

Figure 4. Temporal evolution of G' (a) and G'' (b) for the diblock D78 at $\omega = 0.04$ rad/s at various temperatures after a quench from the disordered state (170 °C).

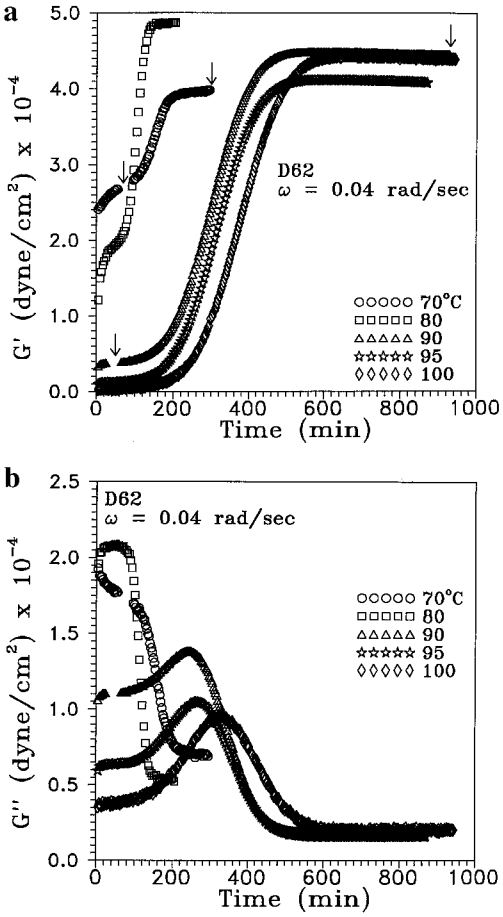

Figure 5. Temporal evolution of G' (a) and G'' (b) for the diblock D62 at $\omega = 0.04$ rad/s at various temperatures after a quench from the disordered state (115 °C). The arrows in part a indicate times at which dynamic frequency scans were performed during the ordering studies.

decreasing T for these polymers[6]) and the retardation of chain mobility that also results from lowering the temperature.

Two other notable features in Figure 4 are the downward slope in G' observed in the quench to 152 °C after 350 min and the much lower long-time value of G' observed in the quench to 154 °C as compared with the other quenches. These effects may result from flow alignment of the lattice at small quench depths, producing an anisotropic material with a lower value of G' in the test direction. Departures from random orientation were also evident in samples run at small quench depths in the SAXS hot stage, as manifested in distortions of the desmeared SAXS profiles (the desmearing procedure assumes random orientation[29]). This orientation, which occurs in the absence of an imposed shear, is presumably induced by the mica windows. Examination of two polymers (D78 ordered at 154 °C in the SAXS hot stage and T149 ordered at 140 °C in the rheometer) by SAXS with an area detector and point collimation (apparatus described elsewhere[32]) revealed some preferred orientation. However, the isotropic component dominated the scattering, so orientation effects were not investigated systematically.

The ordering kinetics for D62 ($T_{ODT} = 110$ °C) shown in Figure 5 are much slower than those for D78 at the same quench depths. This is attributable to the lower temperatures (for the same ΔT) for D62 and the proximity of these temperatures to T_g of the polystyrene domains. Analogous to the D78 data, D62 also shows a minimum in ordering time at 80 °C. Another notable feature of the D62 data at 70 and 80 °C, as well as the D78 data at 110 °C, is the presence of two distinct steps in G' with increasing time. The first step can extend over as much as 40 min (D62 at 80 °C) and thus is *not* due to thermal equilibration of the sample, which is complete in 5 min. The G' ordering curves for the triblock T149 also consist of two segments which are clearly seen for $\Delta T = 24$, 34, and 44 °C in Figure 6. The block copolymers D78 and T149 have similar values of T_{ODT} (see Table 1), so their ordering times may be directly compared; that is, there is no independent influence of the absolute temperature (as when comparing D62 and D78). The increased ordering time for T149 over D78, which is larger by an order of magnitude, certainly reflects the larger molecular weight of the former, although diblock vs triblock architecture may also have some influence on the ordering rate. However, it is interesting to note that the ordering process, as measured by the temporal evolution of G' and G'', follows the same path for diblocks and triblocks; that is, the differences are purely quantitative (with the triblock ordering more slowly), rather than qualitative. Considering the results shown in Figures 4−6, it appears that two distinct steps can be resolved in the ordering curves whenever chain diffusion is sufficiently slow, due either to low temperature (D62) or high molecular weight (T149). Otherwise, only the second step is observable (D78; D90 data not shown).

C. Ordering Kinetics (SAXS). Figure 7 shows the SAXS kinetic results for D62 following a quench to 80 °C. Each scattering profile represents time-averaged scattering over 10 min; the first profile shown was taken at 120 °C, immediately prior to the quench. The peak in the 120 °C profile arises from the correlation hole

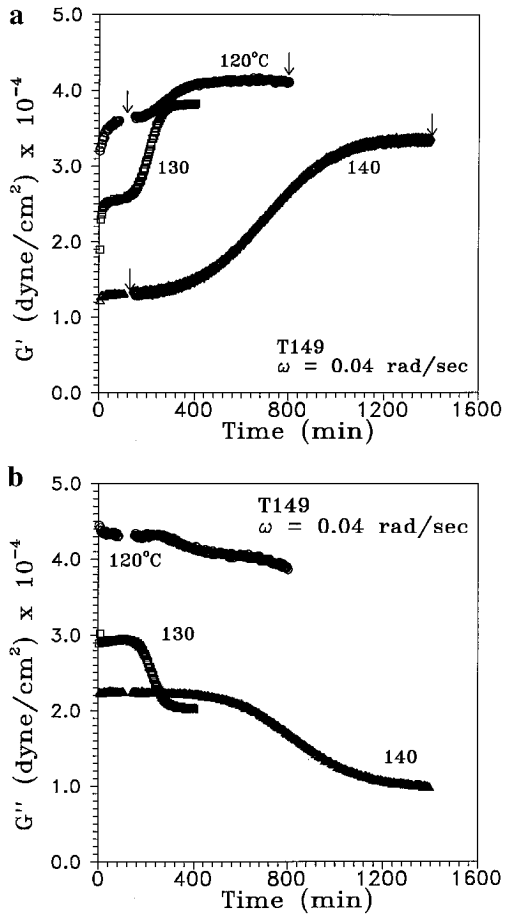

Figure 6. Temporal evolution of G' (a) and G'' (b) for the triblock T149 at various temperatures after a quench from the disordered state (175 °C). The arrows in part a indicate times at which dynamic frequency scans were performed during the ordering studies.

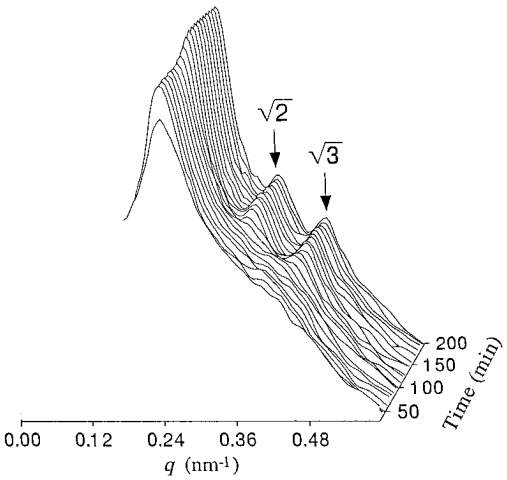

Figure 7. SAXS data for the diblock D62 at 80 °C following a quench from the disordered state (120 °C). Vertical axis is logarithmic in intensity; time = 0 pattern taken at 120 °C. Note the appearance at approximately 100 min of the higher order peaks at positions $\sqrt{2}q^*$ and $\sqrt{3}q^*$ indicative of a body-centered cubic structure.

effect[33] and is considered in greater detail in the Discussion. As the ordering proceeds, the primary peak intensity increases, its width decreases, and higher order reflections develop, while q^* (q position of primary-peak maximum) remains constant. The higher order peaks are located at q positions relative to the primary peak ($\sqrt{2}$, $\sqrt{3}$) that are consistent with the expected bcc lattice structure. The time over which the higher order

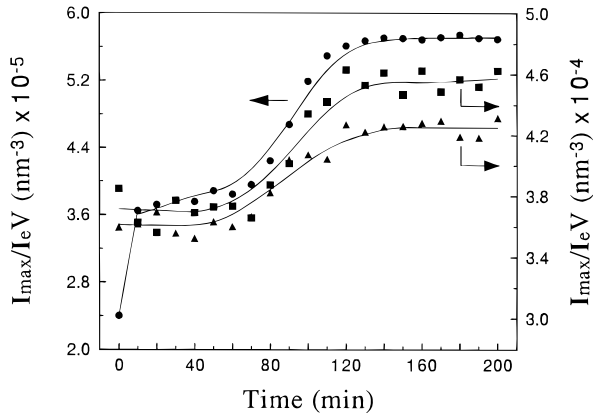

Figure 8. Temporal evolution of the SAXS peak intensities for the diblock D62 at 80 °C after quenching to 80 °C from 120 °C: (●, left axis) primary reflection (at q^*); (■, right axis) peak at $\sqrt{2}q^*$; (▲, right axis) peak at $\sqrt{3}q^*$, intensity multiplied by 1.8. Note that all three peaks develop simultaneously.

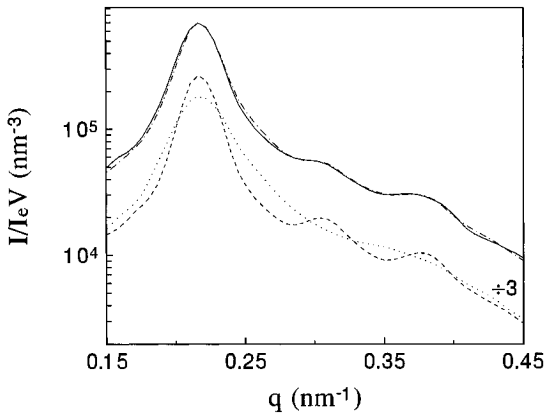

Figure 9. Demonstration that SAXS profiles (T149, 130 °C) at intermediate states during the ordering can be quantitatively represented by a linear combination of profiles before and after ordering. Experimental data: (· · ·) at 30 min, prior to ordering; (- - -) at 600 min, after ordering is complete; (—) at 240 min, roughly halfway into the ordering process. Calculated profile: (— · —) linear combination of experimental 30 min data (weighted 0.43) and 600 min data (weighted 0.57) showing a good match to the experimental data at 240 min. The short- (· · ·) and long-time (- - -) intensities are divided by a factor of three for clarity.

peaks develop is the same as the time span over which the maximum intensity of the primary peak increases from the first to the second plateau value (see Figure 8). The scattering profiles at intermediate times during an ordering run can be described quantitatively by a linear combination of scattering profiles taken at the beginning and the end of the run, consistent with a nucleation and growth mechanism. This is illustrated in Figure 9 for T149 annealed at 130 °C.

The temporal evolution of the primary peak intensity for D62 after quenching from the disordered state is shown in Figure 10. The datum at $t = 0$ represents the intensity in the disordered state at 120 °C, immediately before the quench. As was seen in the rheological results, two distinct plateaus are evident in the SAXS data along with a minimum (at 80 °C) in the ordering time (time necessary for I_{max} of the primary peak to reach its plateau value). Figure 11 shows the SAXS results for T149 annealed at 130 °C, where each scattering profile represents time-averaged scattering over 30 min, and the first profile shown was taken at 180 °C. As with D62, the primary-peak intensity increases from one plateau value to another, the higher order peaks develop simultaneously with the primary-

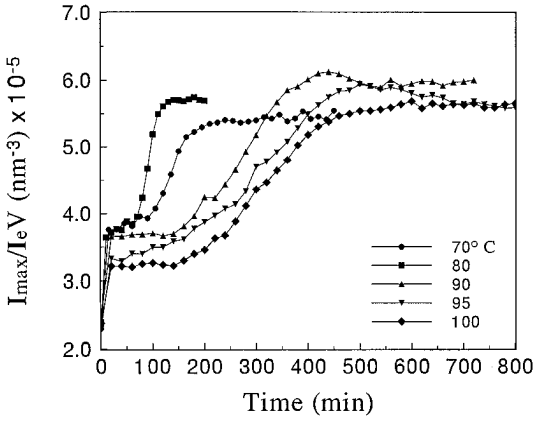

Figure 10. Temporal evolution of the primary peak intensity at different temperatures for the diblock D62 after a quench from the disordered state (120 °C). Time = 0 point corresponds to data at 120 °C.

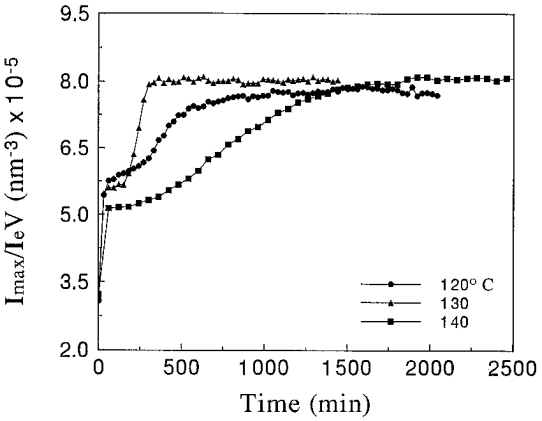

Figure 12. Temporal evolution of the primary peak intensity at different temperatures for the triblock T149 after a quench from the disordered state (180 °C). Time = 0 point corresponds to data at 180 °C.

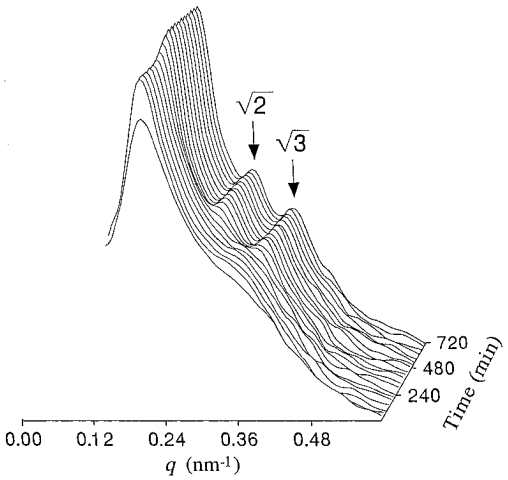

Figure 11. SAXS data for the triblock T149 at 130 °C after a quench from the disordered state. Vertical axis is logarithmic in intensity; time = 0 pattern is taken at 180 °C. Note the appearance of the higher order peaks at positions $\sqrt{2}q^*$ and $\sqrt{3}q^*$ indicative of a body-centered cubic structure at approximately 600 min.

peak intensity, and q^* is invariant with time. Figure 12 shows that the time for the primary-peak intensity to reach its second plateau value displays a minimum at 130 °C, consistent with the rheological results.

IV. Discussion

To facilitate quantitative comparisons of the rheology and SAXS results, half-times ($t_{1/2}$) were extracted from the ordering curves (Table 2). The half-time was defined as the time when G' or I_{max} (height) of the primary SAXS peak reached the arithmetic average of its short- and long-time plateaus after quenches from the disordered state. For the curves that displayed two distinct steps, the second step was used; the first step will be discussed below. As seen in Table 2, the half-times obtained from the two techniques agree well, demonstrating that the same ordering process is being probed by both techniques. This conclusion differs considerably from that reached by Winter *et al.*[20] in their study of an SIS triblock which formed S cylinders in the ordered state. These authors reported an ordering time measured by SAXS which was an order of magnitude shorter than that measured rheologically. They inferred that while SAXS measurements are sensitive to order at the microdomain scale, their rheological measurements were sensitive to the micron-scale grain

Table 2. Ordering Half-times

		$t_{1/2}$ (min)	
polymer	T (°C)	rheology	SAXS
D62	70	165	130
	80	110	90
	90	280	270
	95	320	300
	100	370	310
D78	130	20	
	140	70	
	146	120	
	152	210	
	154	270	
D90	130	<10	
	150	<10	
	170	20	
	180	70	
T149	120	300	370
	130	210	230
	140	720	790
	150	950	
	154	1230	

structure typically exhibited by block copolymers, specifically to the degree of continuity of the styrene cylinders across the domain boundaries. Our materials, which have spherical microdomains, cannot have S-domain continuity across grain boundaries. More work would appear necessary to obtain quantitative relationships between morphology and rheological response.

Comparing our ordering times (Table 2) with those reported by others for near-symmetric SI diblocks,[15,17−19] our asymmetric polymers are much slower to order. Via rheology, Floudas *et al.*[15] measured $t_{1/2} = 5$ min for $\Delta T = 11$ °C on a symmetric diblock ($M_w = 13$ kg/mol) with $T_{ODT} = 86$ °C. By comparison, our D62 has $t_{1/2} = 320$ min for $\Delta T = 14$ °C with $T_{ODT} = 110$ °C—a difference of nearly 2 orders of magnitude for similar values of T_{ODT} and ΔT! Several factors other than T_{ODT} and ΔT may influence the ordering rate, and thus enter into such a comparison: overall molecular weight, polystyrene block molecular weight (through the glass transition temperature of the polystyrene domains formed), and monomeric friction coefficient (through the variation in f). If we assume that the variation in overall molecular weight is dominant, then the ratio of ordering times noted above (320/5) implies that ordering time scales with molecular weight to the 2.7 power. A similar exponent (3.6) is obtained by comparing our data for T149 and D78, which have similar ODT temperatures (Table 1); the half-times for T149 are roughly 10 times longer than for D78 (Table 2). These exponents are

comparable to those found for the molecular weight dependence of the viscosity in entangled polymers (≈3.4), and hence it is tempting to attribute the slower ordering kinetics found for our materials simply to their higher molecular weights and consequently their higher viscosities in the disordered state. However, this implicitly assumes that the rate of molecular diffusion alone controls the rate of transformation from the disordered to ordered states. An additional factor contributing to the ordering rate could arise from differences in nucleation rate between materials. Binder[5] has developed a theory in which the barrier to homogeneous nucleation scales as $|f - 1/2|^5$; the ordering time would thus scale as $\exp(|f - 1/2|^5)$, an extremely strong dependence on asymmetry if indeed the experimental ordering process occurs by homogeneous nucleation. Because our measurements provide only the overall ordering rate, we are unable to discern whether the longer ordering times in the asymmetric case arise from slower growth (due perhaps to molecular weight) or slower nucleation (due perhaps to the asymmetry).

We now return to the question of what the morphology of these materials is during the "first plateau", *prior* to the development of the bcc lattice. As an example, consider the data for T149 at 120 °C (G' data in Figure 6a; SAXS data in Figure 12; first plateau extends from roughly 50 to 300 min). Both methods show a distinct step leading to the first plateau, extending over roughly 50 min; this is far longer than the time needed for thermal equilibration of the sample. From these data, it might be inferred that some sort of morphological change occurs during this first step, prior to the development of true lattice order. One possibility is that during the first step the material microphase separates, producing polystyrene spheres with only liquid-like order;[24] the second step would then represent the ordering of these spheres onto a lattice. Another possibility is that the first step simply represents the time needed for the sample to fully equilibrate at the quench temperature, where it is metastable and subject to large-amplitude composition fluctuations;[17,18,20] since polymer chains must diffuse to form these fluctuations, this equilibration does not occur instantaneously, and its time scale could well exceed the thermal equilibration time when the chain dynamics are slow (close to the polystyrene T_g, for example). These two possibilities might differ in two ways: structural (composition fluctuations and a disordered packing of spheres might have different SAXS patterns) and dynamic (fluctuations are created and destroyed continuously, while microdomains have long lifetimes; if chain exchange between domains is slow in the latter case, differences will be evident in the rheological behavior).

To investigate the morphology present during the first step of the ordering curves, we repeated the rheological ordering study for T149 at 140 °C (Figure 6a) twice more. At a preselected point during each run, the sample was quenched in the rheometer to room temperature and then removed for room-temperature examination by SAXS and tensile testing; the preselected times were 200 min (first plateau) and 1400 min (second plateau). The SAXS pattern for the sample removed during the second plateau (upper curve in Figure 13) shows that the material adopts a well-ordered bcc lattice at long times. By contrast, the pattern for the sample removed during the first plateau (lower curve in Figure 13) indicates substantial disorder and is essentially identical to the SAXS pattern found for T149 immediately after compression molding (prior to annealing). Three prominent features can be seen in the lower

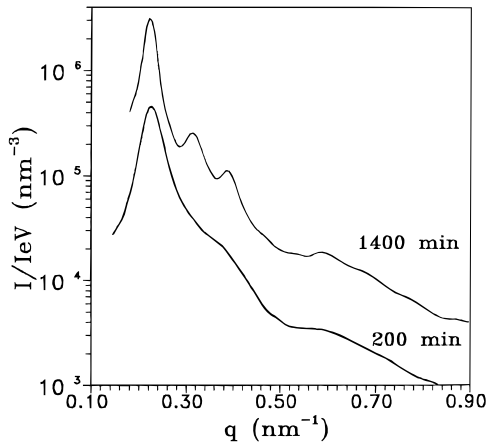

Figure 13. Room temperature SAXS profiles for T149 in the two plateaus of the ordering curve. Samples were heated to 180 °C in the rheometer, quenched to 140 °C and held for variable times, and then quenched to 23 °C for SAXS measurements. Bottom curve: first ordering plateau (200 min at 140 °C). Top curve: second ordering plateau (1400 min at 140 °C) shifted vertically by a factor of 5 for clarity.

profile in Figure 13, a principal peak at 0.22 nm^{-1}, a shoulder at 0.37 nm^{-1}, and a broad maximum at 0.60 nm^{-1}. A quantitative explanation for this type of pattern was given by Kinning and Thomas,[30] who showed that the pattern was consistent with the scattering from an assembly of hard spheres. The principal peak and shoulder result from interference between spheres, while the weak minimum (near 0.52 nm^{-1}) and broad maximum correspond to the first minimum and maximum of the sphere form factor (Rayleigh function). Despite what are clearly large differences in morphology between these two samples, uniaxial stress−strain testing showed essentially identical values of ultimate stress and strain, indicating that the polystyrene end blocks form effective physical cross-links at room temperature in both cases. Thus, both mechanical and SAXS data are consistent with polystyrene spheres being present.

The scattering from disordered block copolymers is generally found to be well represented[13,16−18] by Leibler's RPA theory.[1,41] Note that while the Fredrickson−Helfand[3] treatment of composition fluctuations renormalizes χ compared with the RPA treatment, the *shape* of the scattering curve remains the same: a single scattering peak with no subsidiary maxima. This RPA form thus differs considerably in shape from the scattering expected from an assembly of hard spheres, suggesting that the two possibilities discussed above might be distinguished simply by examining SAXS patterns taken *in situ* during the ordering runs. However, the actual situation is not so clear-cut. Figure 14 shows SAXS data for T149 at 180 °C, 13 °C above its ODT. The solid line is a fit of the experimental data with the polydisperse liquid-like hard sphere model described by Kinning *et al.*;[34] the dashed line is an RPA fit.[41] Although the RPA model does not predict the shoulder, it agrees well in the peak region (see inset in Figure 14, where intensity is plotted on a linear scale). From measurements on D48 ($T_{ODT} \approx 55$ °C) and D62, whose lower transition temperatures permit examination over a wider temperature range in the disordered state, we have found that the RPA fit in the q range above the peak becomes progressively better as $T - T_{ODT}$ increases. The improvement is gradual, however, and deviations are still evident at temperatures as much as 50 °C above T_{ODT}. Such behavior is expected for asymmetric polymers of low molecular weight such as

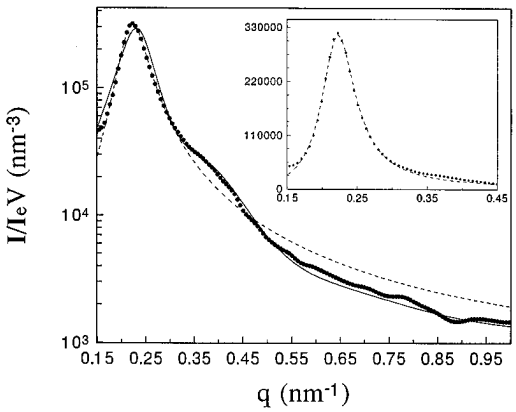

Figure 14. Profile fitting of SAXS data (●) for the triblock T149 measured at 180 °C prior to a kinetic run. The two models used were the random phase approximation (RPA) for disordered triblocks[41] (- - -) and a polydisperse hard-sphere model described by Kinning *et al.*[34] (—) The inset shows the data with the RPA fit plotted on a linear scale. An adjustable background intensity was included in all fits. The following parameters were used in the fits: (a) hard spheres: mean core radius $r = 7.04$ nm, average volume per particle $v = 21\,500$ nm^3, mean hard-sphere diameter $d = 27.1$ nm, and ratio of standard deviation to mean radius $\sigma = 0.244$; (b) RPA: radius of gyration of half the triblock $R_g = 23.7$ nm and Flory–Huggins interaction parameter $\chi = 0.0530$, where the degree of polymerization N is computed by counting each styrene or isoprene monomer as one unit.

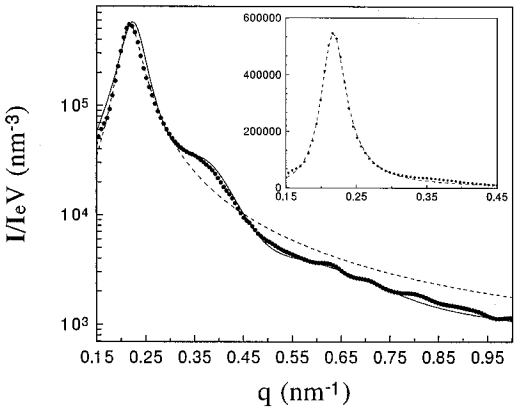

Figure 15. As in Figure 14, profile fitting of SAXS data for the triblock T149 measured during the first 30 min of a kinetic run at 130 °C. The following parameters were used in the fits: (a) hard spheres: $r = 8.22$ nm, $v = 27\,500$ nm^3, $d = 30.5$ nm, and $\sigma = 0.175$; (b) RPA: half the triblock $R_g = 24.2$ nm and $\chi = 0.0533$.

ours where fluctuations are important[3,35] and mean-field behavior is approached only in the high-temperature limit. Put simply, a premise of the RPA treatment is that local composition fluctuations are small. Near the ODT, our polymers are predicted to have[6] $\chi N \approx 60$, which is considerably larger than the value at the mean-field critical point, $(\chi N)_c = 10.5$. Near the ODT, therefore, very asymmetric polymers such as ours should show *large*-amplitude composition fluctuations, which give rise to the structure in the SAXS pattern. The Fredrickson–Helfand treatment also cannot quantitatively describe the fluctuations near the ODT in our materials, which are highly asymmetric and of moderate molecular weight.[3]

Figure 15 shows similar data for T149 taken shortly after the quench to 130 °C (37 °C below the ODT). As shown in Figure 15, the secondary features (shoulder, form factor minimum) are intermediate in prominence between those in the room-temperature (Figure 13, lower pattern) and 180 °C (Figure 14) patterns. Again,

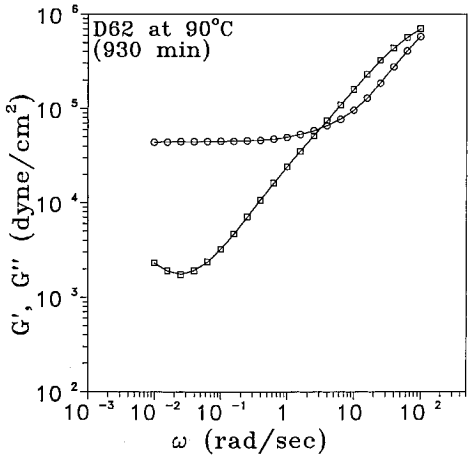

Figure 16. Dynamic moduli, G' (○) and G'' (□), for the diblock D62 as a function of angular frequency at 90 °C during the second plateau of the ordering curve (at 930 min; see arrow in Figure 5a).

the liquid-like hard sphere model qualitatively represents all features of the profile, while the RPA model gives an excellent description of the intensity in the peak region. The resemblances among SAXS patterns at 180 °C and after quenches to 130 °C and room temperature are consistent with a qualitatively similar morphology in all three cases. Thus, we suggest that the "structure" present in the first plateau consists of large-amplitude composition fluctuations, which further develop into the equilibrium structure (spheres on a bcc lattice) in the second step.

The order–disorder transition was originally termed the microphase separation transition (MST) by Leibler,[1] a term which we retained in our earlier work.[6] Our present results highlight some distinctions between microphase separation and ordering, however. Microphase separation—the isolation of blocks into styrene-rich and isoprene-rich domains—occurs in our polymers largely at temperatures *above* T_{ODT}, through the development of large-amplitude composition fluctuations. The high degree of microphase separation which even samples without a lattice order can possess is evident when considering that the specimen yielding the lower SAXS pattern in Figure 13 (which shows substantial disorder) also showed large-deformation stress–strain properties indistinguishable from those of samples showing good lattice order; *i.e.*, the polystyrene-rich domains are sufficiently pure to act as effective physical cross-links at room temperature. Ordering—in our materials, the development of a bcc lattice—is not accompanied here by a substantial change in the extent of microphase separation. Rather, at the ODT, the spatial variations in composition (which are already large in our materials at temperatures just above T_{ODT}) are locked into a persistent pattern, which may be expected to substantially influence the relaxation dynamics.

Rheological measurements can provide information on the dynamics of the structure present during the first plateau. Analogous to the interrupted rheological studies yielding the SAXS patterns in Figure 13, frequency sweeps were performed at selected times (indicated by arrows) for D62 at 70 and 90 °C (Figure 5a) and for T149 at 120 and 140 °C (Figure 6a). For D62 at 90 °C, the moduli during the second plateau (Figure 16) display behavior consistent with a well-ordered bcc lattice structure; *i.e.*, G' is nearly constant at low ω and is much larger than G''. In addition, a minimum in G'' can be seen near $\omega = 0.02$ rad/s. Our studies[36] on these SI and SIS polymers, as well as their hydrogenated

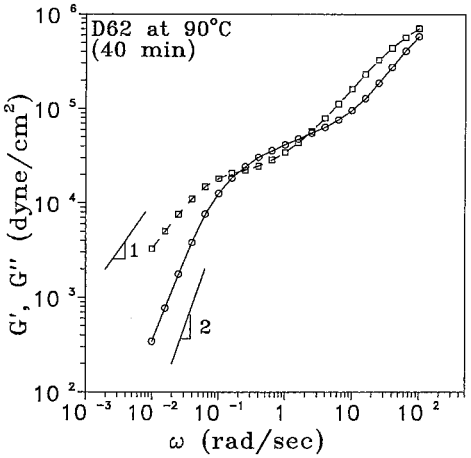

Figure 17. Dynamic moduli, G' (○) and G'' (□), for the diblock D62 as a function of angular frequency at 90 °C during the first plateau of the ordering curve (at 40 min; see arrow in Figure 5a). Note the approach to terminal behavior for both moduli at low frequency.

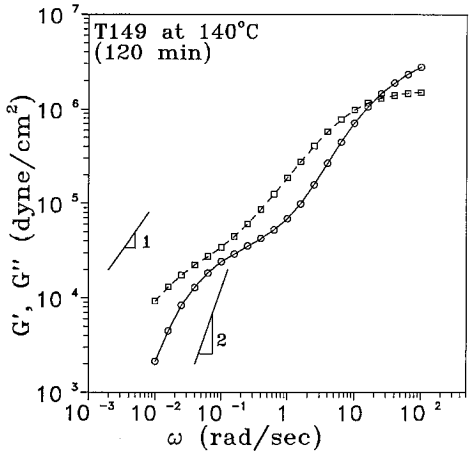

Figure 18. Dynamic moduli, G' (○) and G'' (□), for the triblock T149 as a function of angular frequency at 140 °C during the first plateau of the ordering curve (at 120 min; see arrow in Figure 6a). Note the approach to terminal behavior for both moduli at low frequency.

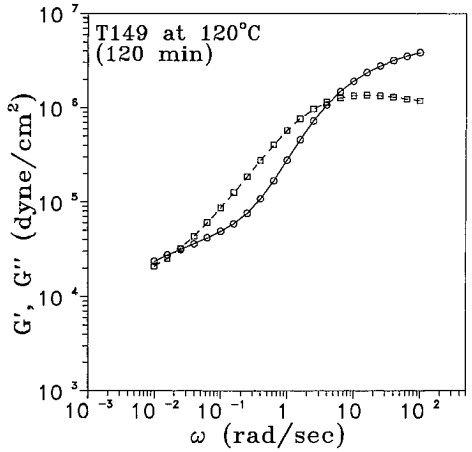

Figure 19. Dynamic moduli, G' (○) and G'' (□), for the triblock T149 as a function of angular frequency at 120 °C during the first plateau of the ordering curve (at 120 min; see arrow in Figure 6a).

derivatives, have shown this minimum in G'' to be a general feature of polymers showing well-developed bcc lattice order. A similar minimum is also evident in data presented by Koppi *et al.*[31] for materials showing a bcc lattice.

The modulus−frequency behavior in the first plateau (Figure 17) is markedly different: at low frequency, G' decreases rapidly with decreasing ω and is smaller than G''. The behavior resembles the response observed[6] at temperatures immediately above T_{ODT}, where terminal behavior ($G' \propto \omega^2$, $G'' \propto \omega$) is obtained, though the terminal region in the metastable state is shifted to lower frequencies. During the first plateau, the diffusion of polymer chains remains relatively rapid, even allowing terminal behavior to be accessed for modest quenches. By contrast, any such relaxation in materials which have adopted the bcc lattice order must be considerably longer (compare Figures 16 and 17). Similar results for T149, taken during the first plateau at 140 °C, are shown in Figure 18. When the material is quenched to lower temperatures, the terminal behavior shifts to frequencies outside the experimental window; data for T149 at 120 °C, taken during the first plateau, are shown in Figure 19. (Frequency sweeps taken for T149 during the second plateau at both 140 and 120 °C are similar to those shown for D62 in Figure 16 and are not shown.)

The time required for composition fluctuations to fully develop (which requires the chains to diffuse roughly one molecular diameter) should be roughly the terminal relaxation time τ_d. Thus, it is worthwhile to estimate τ_d, so that we may compare it with the characteristic time for the *first* step observed in some of the ordering runs. For a polymer in the terminal region, the relaxation time can be calculated from $\tau_d = G'/(\omega G'')$. From the data shown for T149 at 140 °C (Figure 18), $\tau_d = 23$ s during the first plateau, while for D62 at 90 °C (Figure 17), $\tau_d = 11$ s. These values are consistent with the fact that no first step was observed during the corresponding ordering runs (Figure 6a for T149 at 140 °C, Figure 5a for D62 at 90 °C); *i.e.*, the modulus change was complete within the 300 s required to obtain the first data point. By contrast, we can only estimate a lower bound for τ_d in the first plateau shown by T149 at 120 °C, since terminal behavior is not reached (see Figure 19). At the lowest measurement frequency ($\omega = 10^{-2}$ rad/s), $G'/(\omega G'') = 120$ s. However, the true value of τ_d is much larger (perhaps an order of magnitude), since at 10^{-2} rad/s, G' is still larger than G'' and thus the terminal region would not be reached until frequencies which are at least a decade lower. The first step during the T149 ordering run at 120 °C extends for roughly 3000 s (Figure 6a), which is consistent with $\tau_d \approx 10^3$ s. Unfortunately, measurements to lower frequencies are precluded since the time required to make measurements at these lower frequencies exceeds the total time of the first plateau. However, the time scale of the first step appears to be consistent with τ_d during the first plateau, to within the admittedly large uncertainty with which we can estimate τ_d, lending support to our hypothesis that the first step in the two-step ordering curves corresponds to the time required for large-amplitude composition fluctuations to fully develop.

Semenov[37] has developed a theory describing the ordering of spherical microdomains onto a lattice. As noted by Bates and Fredrickson,[38] these microdomains represent large-amplitude fluctuations in an otherwise disordered melt. Because the fluctuations in these asymmetric block copolymers can attain large amplitudes, the styrene-rich regions can severely retard chain diffusion as the glass transition temperature of polystyrene is approached. Thus, the broad transitions we previously reported[6] for polymers which did not show a lattice order correspond essentially to the temperature range over which τ_d changes dramatically due to the

growth of fluctuations. Furthermore, quenching to room temperature drops these regions below their glass transition temperatures, and they can thus serve as effective physical cross-links with essentially infinite lifetimes. From our results, there does not appear to be any significant distinction between large-amplitude composition fluctuations and a disordered arrangement of spheres.

However, distinctions should be drawn between spherical microdomains in block copolymer melts and the more conventional micelles formed by amphiphiles in solution, especially in view of the large body of work done on styrene−butadiene block copolymers in the selective solvent *n*-tetradecane.[22−26,39,40] Neglecting polydispersity, a block copolymer melt contains a single molecular species and thus should exhibit only one phase at an arbitrary temperature and pressure (unless these fortuitously coincide with a phase boundary). Block copolymer solutions, however, are *two*-component systems (again neglecting polydispersity), and thus coexistence of two phases is permitted. Given these qualitative differences between block copolymer melts and solutions, it may not be possible to draw detailed analogies between the two cases.

V. Conclusions

Through the use of time-resolved SAXS and rheological measurements, we have investigated the kinetics of mesophase formation in very compositionally asymmetric styrene−isoprene block copolymers. The ordering half-times obtained from SAXS and rheology are in good agreement; the times and the size of the quench depth that could be probed experimentally are much larger than those reported for nearly symmetric block copolymers. Diblocks and triblocks appear to order by the same mechanism, as judged from the temporal evolution of their moduli and SAXS patterns; however, triblocks order more slowly for similar quench depths and T_{ODT} values. Plots of G' vs time at a fixed frequency contain two steps at low temperatures and/or large molecular weights. The second step corresponds to the development of a bcc lattice of spherical microdomains of polystyrene in a polyisoprene matrix. By contrast, the first step is attributed to the development of large-amplitude composition fluctuations characteristic of the polymer in a metastable state. These fluctuations do not develop instantaneously due to the finite (and, in some cases, slow) diffusion rate of the polymer chains. No clear distinction exists between SAXS profiles taken at temperatures slightly above T_{ODT} and profiles taken in the metastable state below T_{ODT}. These results suggest that the disordered spherical morphology commonly observed in styrenic block copolymers quenched to room temperature may simply result from the vitrification of large-amplitude composition fluctuations.

Acknowledgment. This work was supported by the National Science Foundation, through the Materials Research Group Program (DMR-92-23966), the Princeton Center for Complex Materials (DMR-94-00362), the Polymers Program (DMR-92-57565, to R.A.R.), and a Graduate Fellowship (to J.L.A.). The authors thank Dr. Damian Hajduk for assistance with the SAXS measurements used in assessing preferential orientation of the samples.

References and Notes

(1) Leibler, L. *Macromolecules* **1980**, *13*, 1602.
(2) Mayes, A. M.; Olvera de la Cruz, M. *J. Chem. Phys.* **1989**, *91*, 7228.
(3) Fredrickson, G. H.; Helfand, E. *J. Chem. Phys.* **1987**, *87*, 697.
(4) Fredrickson, G. H.; Binder, K. *J. Chem. Phys.* **1989**, *91*, 7265.
(5) Binder, K. *Physica A* **1995**, *213*, 118.
(6) Adams, J. L.; Graessley, W. W.; Register, R. A. *Macromolecules* **1994**, *27*, 6026.
(7) Chung, C. I.; Lin, M. I. *J. Polym. Sci., Polym. Phys. Ed.* **1978**, *16*, 545.
(8) Gouinlock, E. V.; Porter, R. S. *Polym. Eng. Sci.* **1977**, *17*, 535.
(9) Rosedale, J. H.; Bates, F. S. *Macromolecules* **1990**, *23*, 2329.
(10) Han, C. D.; Baek, D. M.; Kim, J. K. *Macromolecules* **1990**, *23*, 561.
(11) Winey, K. I.; Gobran, D. A.; Xu, Z.; Fetters, L. J.; Thomas, E. L. *Macromolecules* **1994**, *27*, 2392.
(12) Roe, R. J.; Fishkis, M.; Chang, J. C. *Macromolecules* **1981**, *14*, 1091.
(13) Owens, J. N.; Gancarz, I. S.; Koberstein, J. T.; Russell, T. P. *Macromolecules* **1989**, *22*, 3380.
(14) Almdal, K.; Bates, F. S.; Mortensen, K. *J. Chem. Phys.* **1992**, *96*, 9122.
(15) Floudas, G.; Pakula, T.; Fischer, E. W.; Hadjichristidis, N.; Pispas, S. *Acta Polym.* **1994**, *45*, 176.
(16) Floudas, G.; Hadjichristidis, N.; Iatrou, H.; Pakula, T.; Fischer, E. W. *Macromolecules* **1994**, *27*, 7735.
(17) Schuler, M.; Stühn, B. *Macromolecules* **1993**, *26*, 112.
(18) Stühn, A.; Vilesov, A.; Zachmann, H. G. *Macromolecules* **1994**, *27*, 2560.
(19) Hashimoto, T.; Sakamoto, N. *Macromolecules* **1995**, *28*, 4779.
(20) Winter, H. H.; Scott, D. B.; Gronski, W.; Okamoto, S.; Hashimoto, T. *Macromolecules* **1993**, *26*, 7236.
(21) Hashimoto, T. *Macromolecules* **1987**, *20*, 465.
(22) Hashimoto, T.; Kowsaka, K.; Shibayama, M.; Kawai, H. *Macromolecules* **1986**, *19*, 754.
(23) Domany, E.; Nagler, S. *Physica A* **1991**, *177*, 301.
(24) Harkless, C. R.; Singh, M. A.; Nagler, S. E.; Stephenson, G. B.; Jordan-Sweet, J. L. *Phys. Rev. Lett.* **1990**, *64*, 2285.
(25) Singh, M. A.; Harkless, C. R.; Nagler, S. E.; Shannon, R. F., Jr.; Ghosh, S. S. *Phys. Rev. B* **1993**, *47*, 8425.
(26) Shannon, R. F., Jr.; Glavicic, M. G.; Singh, M. A. *J. Macromol. Sci., Phys.* **1994**, *B33*, 357.
(27) Legge, N. R.; Holden, G.; Schroeder, H. E., Eds. *Thermoplastic Elastomers: A Comprehensive Review*; Hanser Publishers: New York, 1987.
(28) Granger, A. T.; Wang, B.; Krause, S.; Fetters, L. J. In *Multicomponent Polymer Materials*; Advances in Chemistry Series 211; American Chemical Society: Washington, DC, 1986.
(29) Register, R. A.; Bell, T. R. *J. Polym. Sci., B: Polym. Phys.* **1992**, *30*, 569.
(30) Kinning, D. J.; Thomas, E. L. *Macromolecules* **1984**, *17*, 1712.
(31) Koppi, K. A.; Tirrell, M.; Bates, F. S.; Almdal, K.; Mortensen, K. *J. Rheol.* **1994**, *38*, 999.
(32) Hajduk, D. A.; Harper, P. E.; Gruner, S. M.; Honeker, C. C.; Kim, G.; Thomas, E. L.; Fetters, L. J. *Macromolecules* **1994**, *27*, 4063.
(33) de Gennes, P. G. *J. Phys. (Paris)* **1970**, *31*, 325.
(34) Kinning, D. J.; Thomas, E. L.; Fetters, L. J. *J. Chem. Phys.* **1989**, *90*, 5806.
(35) Wolff, T.; Burger, C.; Ruland, W. *Macromolecules* **1993**, *26*, 1707.
(36) Adams, J. L. Ph.D. Thesis, Princeton University, 1996.
(37) Semenov, A. N. *Macromolecules* **1989**, *22*, 2849.
(38) Bates, F. S.; Fredrickson, G. H. *Annu. Rev. Phys. Chem.* **1990**, *41*, 525.
(39) Shibayama, M.; Hashimoto, T.; Kawai, H. *Macromolecules* **1983**, *16*, 16.
(40) Shibayama, M.; Hashimoto, T.; Kawai, H.; Watanabe, H.; Kotaka, T. *Macromolecules* **1983**, *16*, 361.
(41) Benoit, H.; Hadziioannou, G. *Macromolecules* **1988**, *21*, 1449.

MA951261+